

10
3/7/89 JGS ①

DR# 0608-4

UCID-21630

Induction Accelerators and Free-Electron Lasers at LLNL

Richard J. Briggs

February 15, 1989

Beam Research Program

Lawrence Livermore National Laboratory

This document contains neither recommendations nor conclusions of the U.S. Department of Energy. It is the property of the U.S. Government, is not subject to copyright protection, and may be reproduced or distributed by the Government or its employees without prior permission or notification. Its use, however, does not authorize anyone to ignore copyright or other intellectual property notices, if any, which may be present in parts of this document that were derived from the work of copyright or other rights holders.

DISCLAIMER

This document was prepared as an account of work sponsored by an agency of the United States Government. Neither the United States Government nor the University of California nor any of their employees, makes any warranty, express or implied, or assumes any legal liability or responsibility for the accuracy, completeness, or usefulness of any information, apparatus, product, or process disclosed, or represents that its use would not infringe privately owned rights. Reference herein to any specific commercial products, process, or service by trade name, trademark, manufacturer, or otherwise, does not necessarily constitute or imply its endorsement, recommendation, or favoring by the United States Government or the University of California. The views and opinions of authors expressed herein do not necessarily state or reflect those of the United States Government or the University of California, and shall not be used for advertising or product endorsement purposes.

Printed in the United States of America
Available from
National Technical Information Service
U.S. Department of Commerce
5285 Port Royal Road
Springfield, VA 22161

<u>Price Code</u>	<u>Page Range</u>
A01	Microfiche

Papercopy Prices

A02	001-050
A03	051-100
A04	101-200
A05	201-300
A06	301-400
A07	401-500
A08	501-600
A09	601

INDUCTION ACCELERATORS AND FREE-ELECTRON LASERS AT LLNL¹

Richard J. Briggs

UCID--21639

Lawrence Livermore National Laboratory

DE89 007691

Livermore, California 94550

ABSTRACT

Linear induction accelerators have been developed to produce pulses of charged particles at voltages exceeding the capabilities of single-stage, diode-type accelerators and at currents too high for rf accelerators. In principle, one can accelerate charged particles to arbitrarily high voltages using a multistage induction machine. The advent of magnetic pulse power systems makes sustained operation at high repetition rates practical, and high-average-power capability is very likely to open up many new applications of induction machines.

In part A of this paper, we survey the U.S. induction linac technology, emphasizing electron machines. We also give a simplified description of how induction machines couple energy to the electron beam to illustrate many general issues that designers of high-brightness and high-average-power induction linacs must consider. We give an example of the application of induction accelerator technology to the relativistic klystron, a power source for high-gradient accelerators.

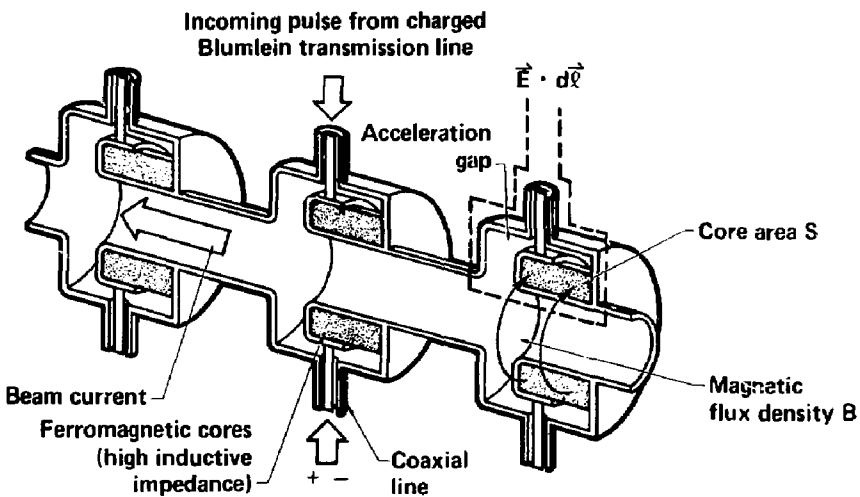
In part B we address the application of LIAs to free-electron lasers. The multikiloampere peak currents available from linear induction accelerators make high-gain, free-electron laser amplifier configurations feasible. High extraction efficiencies in a single pass of the electron beam are possible if the wiggler parameters are appropriately "tapered," as recently demonstrated at millimeter wavelengths on the 4-MeV ELF facility. Key issues involved in extending the technology to shorter wavelengths and higher average powers are described. Current FEL experiments at LLNL are discussed.

PART A: OVERVIEW OF LINEAR INDUCTION ACCELERATORS

Physical Principles of Induction Linac Operation

A linear induction accelerator (LIA) can be thought of as a series of 1:1 transformers in which the electron beam acts as the secondary. A key feature of this configuration is the absence of a "voltage" on any cable or structure that exceeds the voltage supplied to a single accelerator module driven by the pulse source. The electrons, in effect, "integrate" the axial electric field in the vacuum beam pipe to achieve a final energy of n times the module voltage (for n modules.)

These ideas can be more clearly understood by considering the sketch in Fig. 1 of a geometry similar to that of the accelerator modules used at Lawrence Livermore National Laboratory (LLNL). A voltage pulse is supplied to the accelerator module by coaxial cable transmission lines (driven from two sides in a balanced mode to avoid deflection forces on the electron beam). A cylindrical core of ferromagnetic material (for example, ferrite) located in the cavity as shown presents a very high impedance to the drive transmission lines at their junction point with the cavity. With no electron beam present, the "voltage" ($\int E \cdot d\vec{l}$) impressed across the accelerator gap is equal to the transmission line voltage at the junction point with the cavity. This statement is a good approximation only when the pulse length is much longer than the transit time of



$$\oint \vec{E} \cdot d\vec{l} = - \int_S \frac{d\vec{B}}{dt} \cdot d\vec{S}$$

Figure 1. The magnetic induction module.

electromagnetic waves throughout the cylindrical radial line structure (~ 1 ns typically), so the electromagnetic fields can be treated in a quasistatic approximation. Capacitive and inductive effects of the gap, coaxial leads, and other components can particularly affect the electromagnetic field distribution during the rise and fall times of the voltage (beam current) pulse. Note that the electric field in the vicinity of the gap is quasistatic in shape (see sketch in Fig. 1), and there is no coupling of adjacent modules as long as a beam pipe of reasonable length ($>$ pipe diameter) separates the acceleration gaps.

The impedance of the ferromagnetic core will be high for only a limited time, of course, and the "volt-sec" capability of the material determines the core area, S , for a given module voltage and pulse length. Actually, for ferrite-type modules, the manner in which the electromagnetic fields propagate through the ferromagnetic material cannot be ignored, and the ferrite region is often not accurately represented by lumped circuit models. This feature is not crucial for zero-order modeling since the role of the ferrite is to present a sufficiently large impedance to the drive lines, which it does in cases of interest [since $(\mu/\epsilon)^{1/2}$ is large compared to the free-space impedance].

In the presence of an electron beam pulse proceeding down the axis of the accelerator, as illustrated in Fig. 1, a return current in the wall will flow up the gap and "load" the driver transmission line. Once again, this simple picture applies when the current pulse is relatively long (e.g., 50 ns) compared to the transit time of electromagnetic waves up the gap (~ 1 ns).

The pulses are generated with a pulse forming line (PFL); an elementary schematic of such a system is illustrated in Fig. 2. The output of the PFL is applied to the transmission line (in actuality we use a balanced pair of lines to drive the cell.) The transmission lines are long enough to provide "transit time isolation" of the PFL/switch and the cell, that is, the cable transmission time is longer than the pulse length. In this case, the simple equivalent circuit of the drive system shown in Fig. 2 is applicable, where $V_o(t)$ is the pulse waveform supplied to the transmission line by the PFL. The

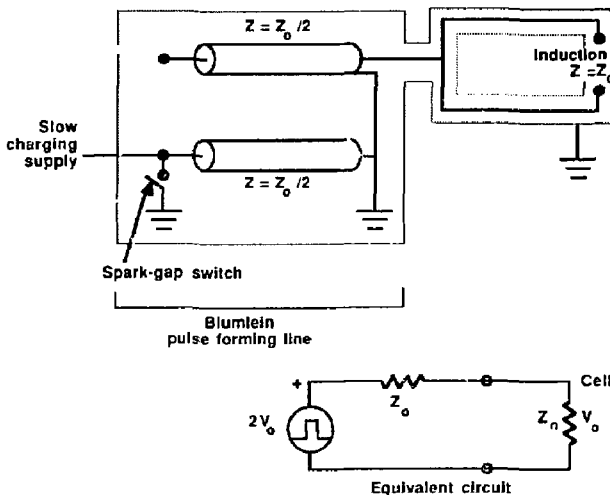


Figure 2. Simplified picture of an accelerator cell driver.

ideal "square wave" shown in the figure is, of course, in practice modified by switch inductances and other factors, which can limit the minimum pulse lengths that have enough of a "flat top" on the waveform to be useful in induction accelerators.

From all these considerations, we can deduce the circuit schematic shown in Fig. 3. The beam current load on the transmission line is accurately represented by a current source because the current is not dependent on the voltage of that stage as it would be in a diode region. External compensation circuits at the transmission line output are often used to help flatten the acceleration voltage pulse and to absorb energy from the transmission lines when the beam is absent (prevent "ringing" of the energy on the cables). In practice, resistors are used on our 50-MeV induction accelerator to absorb half the drive power with a 10-kA beam.

Many observations are readily apparent from this circuit schematic. For example, for optimum efficiency, the transmission line impedance should be matched to the beam impedance, $Z_0 = V_0/I_B$ (in the absence of resistor compensation). Since pulse power system efficiencies can be quite high (up to 60–70% with the latest magnetic modulator systems), induction machines can have good overall efficiencies. Parameter choices can compromise this potential for high efficiency; in particular, with long pulse lengths, compensation for voltage "droop" from finite ferrite inductance in the compensation circuitry will waste some drive current.

This simple schematic also shows the difficulty in avoiding beam energy variation in the head and tail of a heavily loaded (relatively efficient) induction machine, where I_B is changing. Matching $V_0(t)$ and $I_B(t)$ waveforms is possible in principle but difficult in practice. As a consequence, beam transport systems in induction machines must often accommodate a relatively broad energy variation through the electron beam pulse. Difficulties with our 50-MeV machine, for example, have often been traceable to the problems of handling a time-varying energy on the beam head.

High-Brightness Electron Beams

Over the past two decades, LLNL and the Lawrence Berkeley Laboratory have collaborated on the development of several LIAs. These include the Astron (6 MeV,

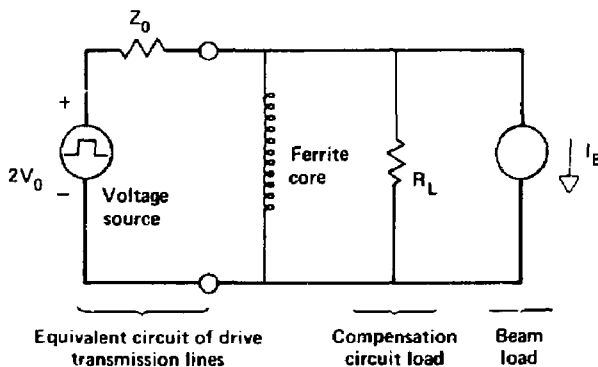


Figure 3. Simplified schematic of induction unit.

0.5 kA, 300 ns), the ERA (4 MeV, 1.5 kA, 30 ns), the Experimental Test Accelerator (ETA) (5 MeV, 10 kA, 30 ns), and the Advanced Test Accelerator (ATA) (50 MeV, 10 kA, 70 ns). When these accelerators were developed, the primary requirement was to achieve high beam currents with relatively little concern for beam emittance. The free-electron laser (FEL) application for LIAs, in contrast, places a very high premium on beam brightness and on high-average-power operation. The technology for these requirements was developed on our Accelerator Research Center (ARC) accelerator (2 MeV, 0.8 kA, 50 ns, and multikilohertz repetition-rate capability). The brightness of an electron beam (the beam's density per unit 4-volume of phase space, V_4) is defined as

$$J = I/(\gamma\beta)^2 V_4 , \quad (1a)$$

$$J[A/(m\text{-rad})^2] = \Psi I/(\pi\epsilon_n)^2 , \quad (1b)$$

where I is the beam current, ϵ_n is the normalized edge beam emittance ($\beta\gamma RR'$), and Ψ is a shape factor (for uniform density ellipsoids in phase space, determination of edge emittance specifies $\Psi = 2$). Using conservation of momenta ($m_0 v_{(\text{source})} = \gamma m_0 v_{\perp}$) and $\beta = v_z/c$, we can describe the lower bound on beam emittance as it leaves a "perfect" (smooth and uniformly emitting) cathode plane of temperature T_e and radius R :

$$\begin{aligned} \epsilon_n &= \beta\gamma R R' = \beta\gamma R \frac{V_{\perp}}{V_z} = R \frac{V_{(\text{source})}}{c} , \\ &= 0.2 R_{\text{meters}} \sqrt{T_e(\text{eV})} . \end{aligned} \quad (2)$$

Obviously, the "perfect" cathode source for high brightness requires a low effective temperature and a high extraction-current density (small radius). Researchers in our injector development program, in which the goal is to develop a 3-kA beam with normalized brightness of $2 \times 10^9 A/(m\text{-rad})^2$ to meet our FEL requirements, have explored various cathode technologies to quantify these operating parameters. Of equal importance, we are trying to determine how requirements of continuous high power and high-repetition-rate operation compromise the performance of various cathodes. In Table 1, we briefly summarize our findings. As is apparent from Table 1, we are concentrating on the dispenser cathode primarily because it is best able to generate the high-brightness beams and satisfy the reliability requirements of high-average-power, high-repetition-rate operation.

The operating parameters of a high-current/high-brightness injector are determined by the following two requirements, which incorporate the criteria set by preservation of the normalized cathode emittance in the subsequent transport and acceleration processes:

1. The extraction electric field E ($= V/d$, where V is the injector voltage and d is the cathode-to-anode gap spacing) has a practical upper limit if one is to prevent unwanted emission from noncathode surfaces. Even modest electron emissions from such regions, when combined with those originating from the cathode, drastically increase emittance and make management of stray power very difficult in high-average-power operation. Our initial high-average-power tests at full repetition rates indicate that, for satisfactory operation, E must be limited to 120 kV/cm.

Table 1. Study of cathodes for high-brightness and high-average-power operation.

<i>Cathode type</i>	<i>Description</i>	<i>Summary</i>
Plasma surface discharge	Many small sites of surface electrical discharge; energy per discharge site is low and controllable	<ul style="list-style-type: none"> Good current density ($>20 \text{ A/cm}^2$) and uniformity Rugged and reliable repetition-rate operation Poc; beam emittance due to granularity and high effective temperature of emitting plasma sheath
Field emission	Surface ionization and/or whisker vaporization forms cathode plasma	<ul style="list-style-type: none"> Good current density Dense plasma closure of anode-cathode gap limits repetition rate Emittance and uniformity uncertain Degrades under high-average-power operation
Occluded, gas-enhanced field	Velvet cloth as large surface area gas source with fibers giving field enhancement	<ul style="list-style-type: none"> Good current density (50 A/cm^2) Uniformity of emission degrades with lifetime Beam brightness $\text{few} \times 10^5$ Plasma closure limits repetition rate
Thermionic emitters	Low work function triple-oxide coatings on heated surfaces	<ul style="list-style-type: none"> Limited current density ($\sim 10 \text{ A/cm}^2$), but with good uniformity; beam emittance unknown Taxing vacuum requirements and highly susceptible to poisoning Thermal stresses weaken bond of oxide to supporting substrate Not mechanically reliable under high-power operation
LaB_6	Low work function material heated to very high temperatures (2400 K)	<ul style="list-style-type: none"> Good current density (50 A/cm^2) and uniformity, emittance unknown Very delicate to thermal stresses High-average-power operation untested
Dispenser	Low work function barium-impregnated surfaced heated elevated temperature ($\sim 1100 \text{ K}$)	<ul style="list-style-type: none"> Good current density (20 A/cm^2) and uniformity Beam brightness $> \text{few} \times 10^6$ Reliable operation at full repetition rate Taxing vacuum requirements
Photo-emission	Laser-irradiated surface	<ul style="list-style-type: none"> Untested, known to have good current density and uniformity, but total current and charge (surface area and pulse duration) are limited Testing for high-repetition rate operation requires major investment in laser development

2. Increases in beam emittance during transport stem from the coupling of space-charge fields to the beam-particle trajectories. Beams with uniform profiles minimize this coupling. For uniform cathode emission, the ratio of cathode radius, a , to gap spacing, d , appears to have a limiting value, which, from extensive numerical simulation, we estimate to be $\leq 1/3$. These simulations seek to optimize beam parameters of cathode radius, gap spacing, anode bore size (that is, the effective size of the hole in the anode through which the beam is extracted), the z-variation in transport axial magnetic field (to avoid angular momentum, the axial magnetic field is zero on the cathode surface and then increases to full focusing strength), the injector voltage, and geometric shapes of all cathode-anode-electrode components.

The total beam current is determined by $I = \pi a^2 j$, where j is the current density (assumed to be uniform according to requirement 2). Note that

$$j = K (\gamma) \frac{V^{3/2}}{d^2} , \quad (3)$$

where K is the perveance, which includes relativistic and anode-depression corrections.

To explicitly display the limiting parameters, we write the current as

$$I = \left[\pi K \left(\frac{a}{d} \right)^2 E^{3/2} \right] d^{3/2} . \quad (4)$$

This result numerically implies that if 3 kA is the desired beam current, gaps of 25 cm driven at 3 MeV are required. Using dispenser cathodes, the ARC facility operates at high average powers with the following performance parameters:

- Beam current 0.8 kA.
- Injector voltage 0.8 MeV.
- Post acceleration 1.2 MeV.
- Beam brightness measured at 2.0 MeV was 1.3×10^9 A/(m-rad)².

Future research will be directed toward developing higher voltage (3 MeV) injectors, which will allow increased beam current. Work will continue at the ARC facility and on our new, upgraded ETA accelerator (ETA-II). ETA-II began operation in November, 1987, with a 1-kA, 7-MeV, 50-ns electron beam of high brightness [1.3×10^9 A/(m-rad)²] at a 1-Hz repetition rate. An eventual goal is 3 kA at 2×10^9 A/(m-rad)² brightness at repetition rates up to 5 kHz.. The purpose of ETA-II is to integrate all aspects (physics and engineering) of high-average-power, high-brightness electron beam accelerators into one test facility.

High-Average-Power Technology

The generation of intense, relativistic electron beams requires low-impedance, pulse-compression devices to provide the short (70-ns) acceleration voltage pulse. The spark-gap-based system has served us well on both the ETA and ATA accelerators. However, even during the construction of the ATA accelerator, we recognized that the limitations of spark gaps in repetition rates (duty factor) and reliability would not allow us to apply this technology to high-average-power systems.

During construction of ATA, we worked to find a longer term replacement for the spark-gap-driven Blumlein that could be used on the new device. This effort was

accelerated when we began the FEL program. FEL applications place very stringent requirements on the power-conditioning systems. Those requirements drive us toward higher repetition rates, higher efficiency, better energy regulation during the acceleration pulse, and higher accuracy in alignment of components.

To generate the required 10-GW acceleration pulse for near-term systems, we are using the well-tested magnetic pulse compressor, MAG-1-D. Although this pulse-compression scheme has been around for a number of years, only recent advances in magnetic materials and technology have allowed us to use it to generate nanosecond pulses with efficiencies exceeding 90%. This technique uses the large changes in permeability exhibited by saturating ferromagnetic materials to produce large changes in impedance. We use state-of-the-art switches (thyatrons, silicon-controlled rectifiers) to initiate the pulse at the 100-MW level and to compress it to the 10-GW levels required by the accelerator. Because the compressor uses strictly passive devices (inductors and capacitors), when properly designed its lifetime exceeds 10^9 cycles.

The current magnetic-drive system is shown in Fig. 4. It consists of an intermediate store switch chassis (ISSC), a precompression stage, a step-up transformer, the first stage of compression, and the final stage of compression. The final stage delivers energy from the PFL to the accelerator in the form of a 70-ns pulse at 125 kV through two 4Ω lines. The various waveforms in the MAG-1-D are shown in Fig. 5.

This system has been used during the past two years to generate the high voltages required by the ARC injector for studies of high-brightness, high-current beams. The beam from the injector was accelerated through two ten-cell modules (Fig. 6) for a total energy of 2-3 MeV at the point where the brightness measurements were performed.

The stringent peak-power and repetition-rate requirements are stressing the capabilities of current state-of-the-art thyatrons. To date we have achieved 2.5-kHz repetition rates at nearly full-power output. To reach our goal of 5 kHz, we are experimenting with the "Gatling-gun" mode of operation, where two ISSCs are fired in sequence at 2.5 kHz. We will apply this idea in our new ETA-II high-average-power accelerator.

The magnetic power systems described here should make linear induction accelerators available for many applications in the future, including

- E-beam drivers for microwave and millimeter wave sources.
- Fusion plasma electron cyclotron heating current drive with a 1-2-mm-wavelength FEL.
- E-beam driver for infrared to visible-wavelength FELs.
- The two-beam accelerator.
- The relativistic klystron.
- E-beam driver for collective accelerators.
- Radiation processing.

Using induction accelerators for radiation processing is, in one sense, the least obvious application to consider since a high-peak-current capability is not required. Nonetheless, the "rugged" nature of this solid-state pulse power technology, the system simplicity (for example, modest vacuum requirements) made possible because of the very short duration of the high-voltage pulses, and the relatively low cost per watt do warrant serious examination of its applicability, even for applications requiring low peak currents.

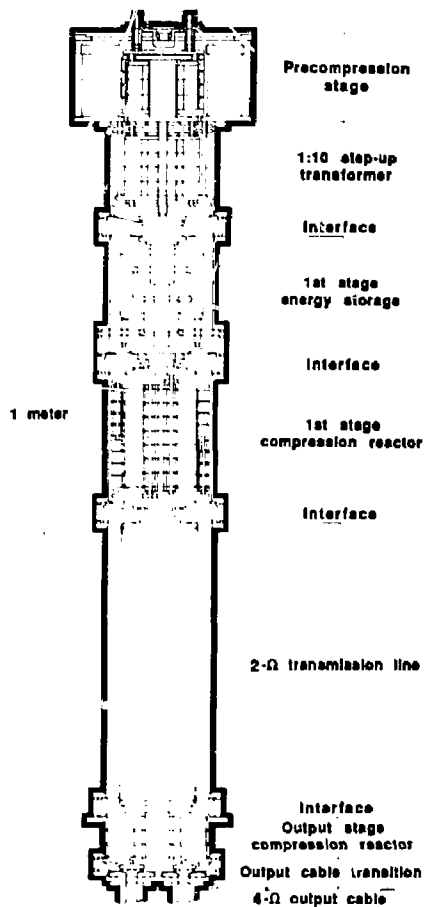


Figure 4. MAC-1-D power compressor.

Application of Induction Accelerator Technology to High-Gradient Accelerators

We would like to discuss, as one example of the applications mentioned above, recent research at LLNL on the relativistic klystron. This work is a collaborative effort with the Stanford Linear Accelerator Center and the Lawrence Berkeley Laboratory.¹

Relativistic klystrons are being developed as a power source for high gradient accelerator applications which include large linear electron-positron colliders, compact accelerators, and FEL sources. These applications require a new generation of high gradient accelerators. Conceptual designs for large linear electron colliders for research at the frontier of particle physics, for example, call for center-of-mass energies of

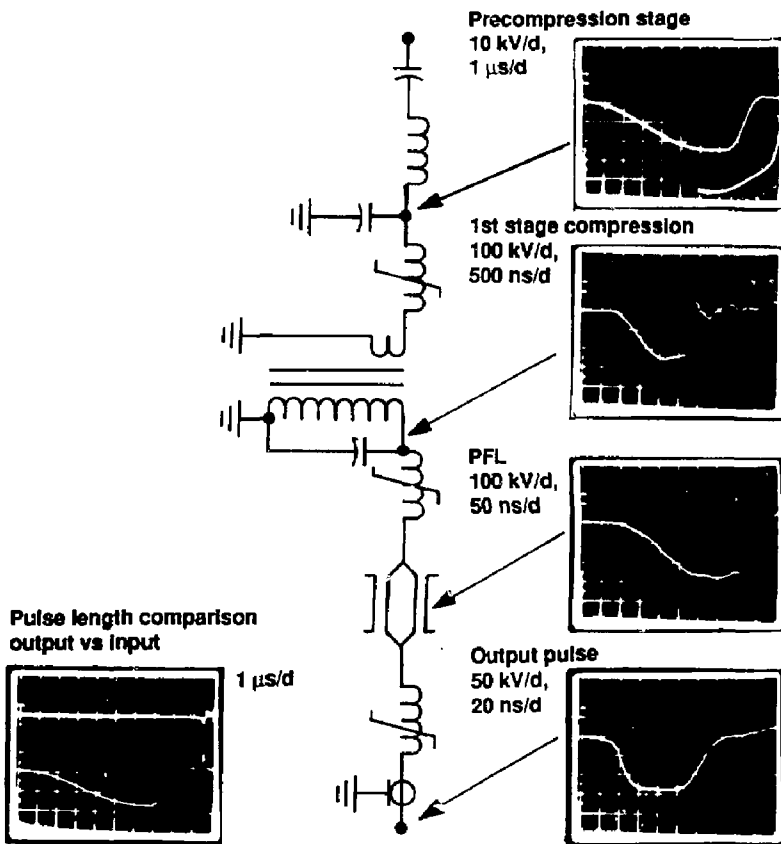


Figure 5. MAG-1-D voltage waveforms.

1–2 TeV. Accelerating gradients of 150–200 MV/m are desired in order to keep the accelerator length within acceptable limits. Frequencies of 11–17 GHz are desired in order to keep peak power requirements and beam loading reasonably small. The peak power necessary to drive a traveling wave structure in the desired frequency range with the desired gradient is of order 1 GW/m with a pulse length of 50–100 ns.

Pulsed beams of such high peak power can be obtained using the technologies of magnetic pulse compression and induction acceleration (see Fig. 7). Beam pulses of 1 kA current and 50–100 ns duration are routinely accelerated to several MeV at LLNL. These beams contain several gigawatts of peak power, as we have discussed earlier.

A. M. Sessler and S. S. Yu, following a suggestion by W. K. H. Panofsky, proposed a direct method for energy extraction from an electron beam by bunching a relativistic beam and passing it through extraction cavities. They suggested that if only part of the beam energy were extracted, the beam could be reaccelerated and energy

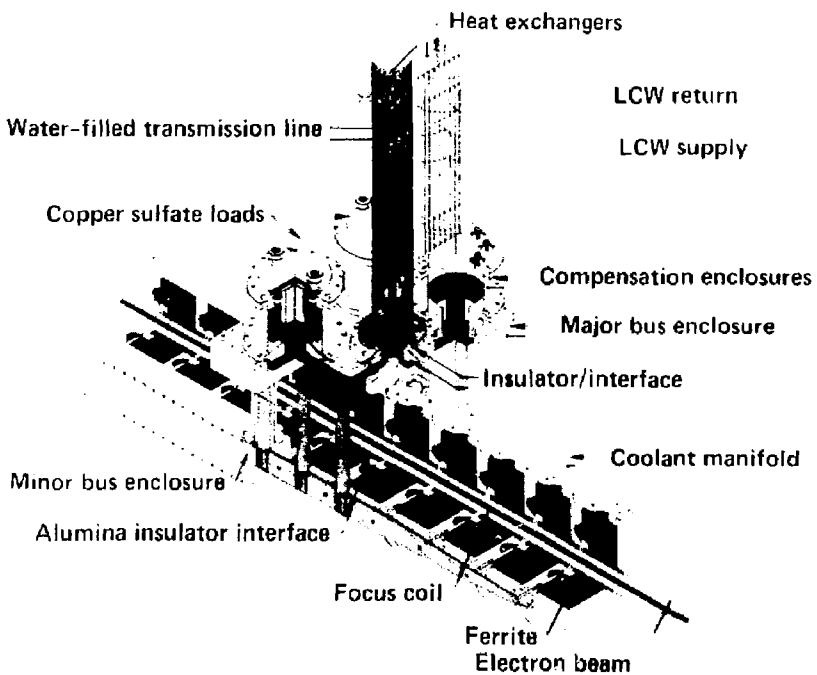


Figure 6. Ten-cell induction accelerator module on ARC.

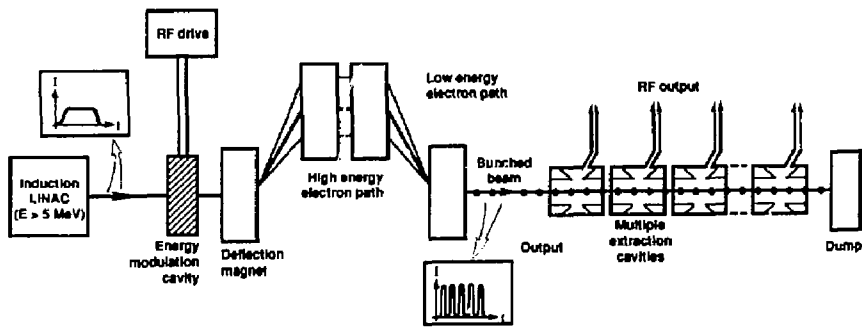


Figure 7. Schematic of a relativistic klystron.

again could be extracted. Repeated reacceleration and extraction was the concept they called a "relativistic klystron two-beam accelerator" (see Fig. 8).⁷ The idea of a relativistic klystron, however, is not limited to the two-beam accelerator concept. Relativistic klystrons can be imagined which span the range from a 1-GW device powering 1 m of accelerator, to a 10-GW device powering 10 m, to a two-beam device extending several kilometers.

Our first experiments have been done at our ARC facility using as a gun an induction accelerator designed to produce 1-kA currents with 1.2-MeV kinetic energy for up to 75-ns duration. Three different klystrons have been tested with this injector. They have operated at 8.6 and 11.4 GHz.

In one experiment we achieved a peak output power of 200 MW at 11.4 GHz from one of our relativistic klystrons. We used a 930-kV, 420-A electron beam from the induction injector. The 200-MW peak power was delivered by this klystron to a 26-cm-long high gradient accelerator structure and corresponds to a longitudinal accelerating gradient of 140 MV/m. We are currently trying to understand the rf pulse shapes that were produced, as the rf flat top was much shorter than the beam current pulse, and this shape was not predicted by our numerical simulation. Experiments are continuing on different cavity geometries.

Our goal is to develop a high power (500 MW), short wavelength (2.6 cm) relativistic klystron driven by an electron beam from an induction accelerator at an energy greater than 1 MeV.

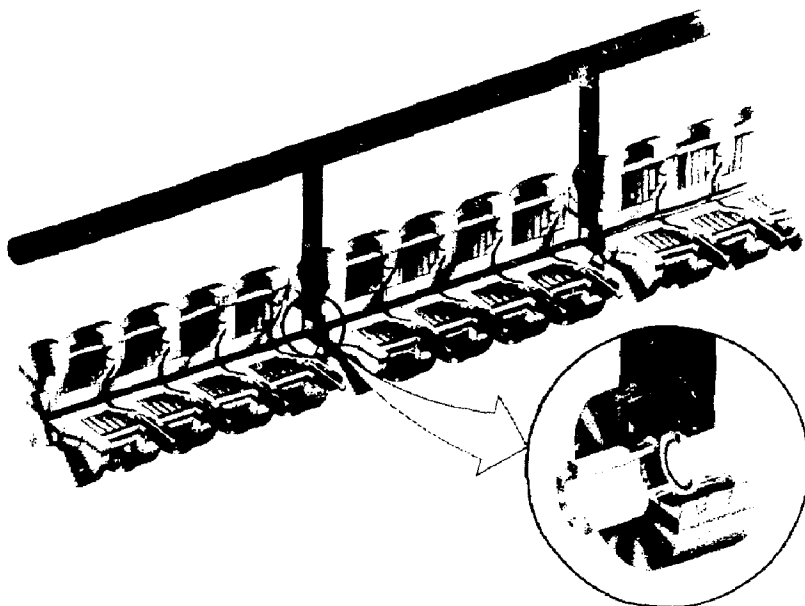


Figure 8. Relativistic klystron version of a two-beam accelerator.

PART B: OVERVIEW OF FEL DEVELOPMENT WITH INDUCTION LINACS AT LLNL

Introduction

Induction linacs are capable of producing multikiloampere peak currents. This capability has stimulated the investigation of single-pass free-electron laser (FEL) amplifiers with very high gain and high conversion efficiency. Experiments on the tapered wiggler concept for achieving high conversion efficiency met with dramatic success on the 35-GHz microwave experiments with the Electron Laser Facility (ELF) at LLNL.³ Current efforts are focused on extending these results to much shorter wavelengths with the 50-MeV PALADIN experiments on our Advanced Test Accelerator (ATA).

An overview of the induction linac-based FEL master oscillator-power amplifier (MOPA) is given in the next section. The fundamental physics issues involved in the tapered wiggler operation are described in the following section, with particular emphasis on explaining the requirements of small electron-beam energy spread and high brightness for efficient energy conversion.

General Description of Induction-Linac Powered FEL Amplifiers

A schematic showing the various elements of a single-pass MOPA FEL configuration driven by an induction accelerator is presented in Fig. 9. The induction accelerator is basically a linear series of pulse transformers that individually give an increment of voltage to the electrons as they pass down the axis of the system. The pulse lengths of the acceleration voltage are generally chosen by compromising between the desire to minimize the magnetic material volume (volt-sec) and the need to maintain an adequate flat top on the acceleration waveform, as we have discussed in Part A. These compromises result in pulse lengths of 50–70 ns in current systems. High average power is obtained by operating at high pulse-repetition rates; the magnetic modulator system is the technology that will enable us to meet this objective.

The electron-beam pulses from the accelerator are sent through the wiggler and discarded in a beam dump. A drive laser (or microwave source) sends input pulses in synchronism with the driving electron-beam pulses. The front section of the wiggler has uniform properties, acting as a linear amplifier (a "preamp") for the input laser. The electromagnetic power increases exponentially with distance up to the point where the electrons are "trapped" by the wave—at this point the electron beam is strongly bunched in "pancakes," periodic at the input signal wavelength (Fig. 10). Beyond this point, the wiggler properties must be tapered with distance to extract a significant fraction of electron-beam energy (tens of percent), as explained in the next section.

Radiation from the "pancake bunches" of relativistic electrons is highly peaked in the forward direction because of the usual relativistic dipole radiation pattern (cone of angle $\sim 1/\gamma$) and also because the individual electron's dipole radiation is also summed over the "pancake" of radial width $d \gg \lambda$, thereby acting like a "forward-fire" phased-array antenna. The overall result is that the FEL gain pattern is highly peaked in the forward direction. Many of the usual limitations on the maximum gain per module do

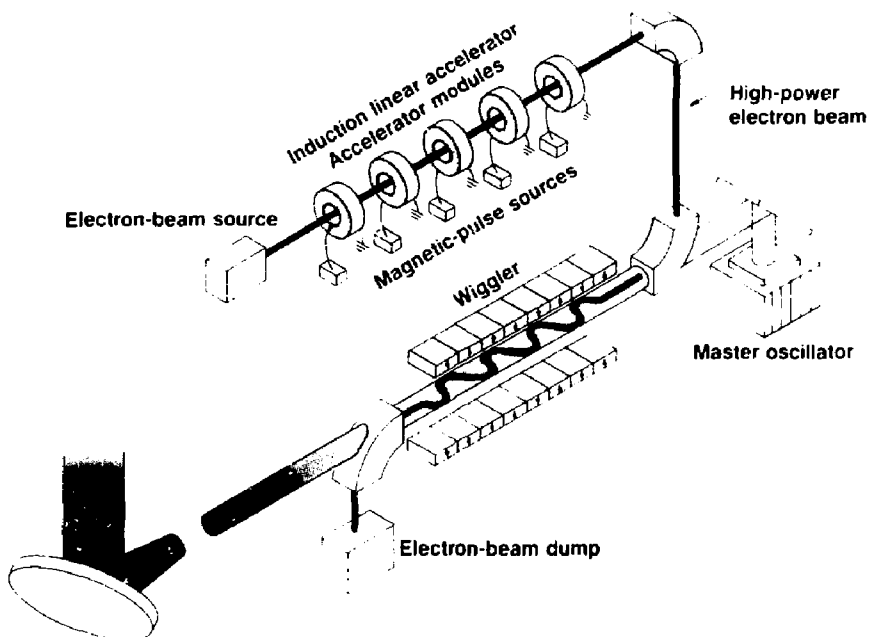
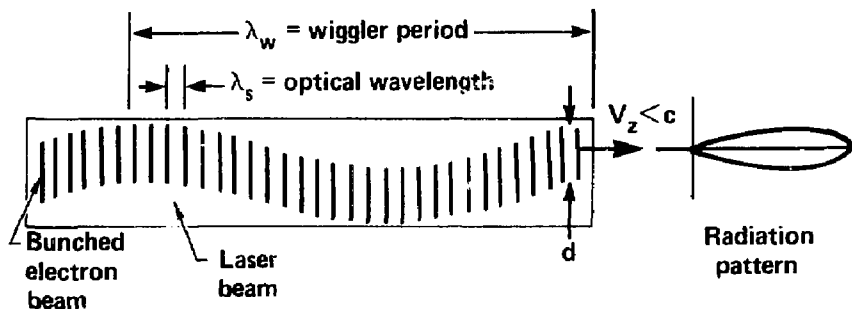


Figure 9. Component technologies for induction linac FEL amplifiers.



- Electron bunches "slip" one optical period per wiggler wavelength relative to light beam
- "Slices" of laser and electron beam $N\lambda_s$ long interact independently (N = number of wiggler periods)
- Radiation of bunched beam is strongly peaked in forward direction (like a "phased array" of radiating dipoles of width $d \gg \lambda_s$)

Figure 10. Schematic of FEL amplifier operation.

not apply to the FEL, because oscillations from "spurious modes" with transverse gain are absent. The pulsed nature of the driving electron beam also simplifies greatly the handling of reflections in FEL amplifiers with very high gain. The experimentally demonstrated capability for 80-dB small-signal gain in the millimeter wavelength experiment (ELF) without spurious oscillations is noteworthy in this context. (We should note that growth of sideband frequencies that couple to the axial oscillations of electrons trapped by the wave is one of the few spurious modes of potential significance in this laser system.)

The optical beam output from the FEL amplifier can be expanded to a low enough power density for beam transport and beam directors to handle, even with the very high average powers that can be achieved at high repetition rates. In microwave systems it is not necessary to have output windows (in applications such as plasma heating or driving rf accelerators) because sensitive components like the electron cathode are physically well isolated from the output waveguide.

The fundamental characteristics of induction-linac-driven amplifiers are well suited for applications requiring very high peak and/or average power outputs from a single aperture. Electron beams of high power can be generated quite efficiently, and the "gain medium" consisting of electrons, dipole wiggler fields, and a vacuum pipe presents very few limitations on power or power density in the gain region.

FEL Amplifier Physics

The proper operation of an FEL amplifier requires that one maintain a precise relationship between the longitudinal velocity of the electron beam and the wavelengths of both the electromagnetic radiation and the wiggler's magnetic field. This relation is given by

$$\gamma_{\parallel} = \left(\frac{\lambda_w}{2\lambda_s} \right)^{1/2} \pm \delta , \quad (5)$$

where λ_s is the wavelength of the electromagnetic wave to be amplified, λ_w is the period of the wiggler, and γ_{\parallel} is defined by

$$\gamma_{\parallel}^2 = \frac{1}{1 - v_{\parallel}^2/c^2} , \quad (6)$$

with v_{\parallel} the longitudinal (axial) velocity of the electrons. The quantity δ represents the accuracy to which the electron's longitudinal energy must be held if a significant transfer of energy from the electron to the electromagnetic wave is to take place. Limits on δ depend on both the intensity and the wavelength of the light to be amplified, and these limits can range from a few percent at microwave wavelengths to a few tens of percent at optical wavelengths.

If an amplifier is to be efficient, a very high quality electron beam is required so that all electrons within the beam satisfy Eq. (5). This not only implies careful control of the beam energy, but, in addition, mandates careful control of the beam's emittance

(ϵ_n). One can estimate the emittance requirement by relating the emittance to the dispersion in axial velocities, which can be written as

$$\frac{\Delta Y_{\parallel}}{\gamma_{\parallel}} = \frac{b_w \epsilon_n}{4(1 + a_w^2)}, \quad (7)$$

where $b_w = eBmc$, with B the peak wiggler magnetic field, and $a_w = \frac{b_w}{\sqrt{2}k_w}$, the rms dimensionless vector potential with k_w the wiggler wave number.

Once the electron beam requirements are satisfied, one is left with the problem of extracting large amounts of energy from the electron beam (several tens of percent) under the constraints of Eq. (5). Obviously if the longitudinal velocity, v_{\parallel} , changes substantially as a result of electron beam energy loss, according to Eq. (5), the interaction will cease, and the amplifier will saturate before significant energy extraction has occurred. A method for circumventing this limitation was first described by Kroll, Morton, and Rosenbluth⁴; it is called the tapered wiggler.

The tapered wiggler concept relies on having the wiggler properties vary as the electrons slow down, so that the resonance condition can be preserved while extracting large amounts of energy. The simple realization of this concept would be to decrease λ_w proportional to γ_{\parallel}^2 , but operationally it is difficult to build wigglers with the requisite short periods at the downstream end. If one recognizes that

$$\gamma_{\parallel} = \frac{\gamma}{\left[1 + 1/2(b_w/k_w)^2\right]^{1/2}}, \quad (8)$$

however, one can see that the electron's total energy (γ) can be reduced without altering its parallel energy (thus maintaining resonance) by simultaneously reducing the wiggler's magnetic field, b_w . This is the approach taken in the design of our wigglers at LLNL.

ELF, a microwave FEL, was specifically designed to test the tapered wiggler concept. The ELF experiments showed that untapered efficiencies of 5-6% could be increased to 40% by appropriately tapering the profile of $b_w(z)$, in good agreement with the modeling. Also ELF has shown high exponential gain (in the small-signal regime) in accordance with theoretical predictions. Utilizing tapered wigglers, these experiments demonstrated high gain (greater than 42 dB) even when operating at high power levels, i.e., one can make the transition from small signal gain to large signal gain in a single device.

ELF is unable to test certain aspects critical to the operation of an optical FEL. First, one must change the method of transporting or focusing the electron beam in the wiggler. Quadrupoles (as used on ELF) would cause a loss of efficiency. Curved pole pieces are essential for operation of a linearly polarized wiggler and are incorporated on the 10.6- μm wavelength PALADIN experiment at ATA.

Second, ELF is a microwave amplifier operated in a waveguide; therefore, it is unable to address the questions of optical guiding and optical mode control that are being addressed on the PALADIN experiments.

In summary, ELF has demonstrated the validity of the tapered wiggler concept. The PALADIN experiments currently under way are intended to show that those concepts are also valid at optical wavelengths.

High Brightness and High Average Power

The FEL application using linear induction accelerators places a very high premium on electron beam brightness and on high-average-power operation. A discussion of both these topics has been given in part A, "Overview of Linear Induction Accelerators."

FEL Experiments at LLNL

Our first FEL experiment, completed about two years ago, involved a 4-MeV, high power, pulsed electron beam from our ETA accelerator. The master oscillator was a 35-GHz microwave source coupled to the electron beam at the entrance to the wiggler. Figure 11 shows the 3-m wiggler with the waveguide and external quadrupole magnet coils for guiding the electron beam. Some results from this experiment are given in Fig. 12. The main conclusions from these experiments were that the feasibility of the basic FEL concept described above was confirmed, and that our theoretical models were accurately predicting performance of these high-gain amplifiers. Further discussions of results from these experiments are given in Ref. 3.

The extension of FEL amplifier operation to the optical regimes requires higher voltage accelerators, and wigglers of many tens of meters in length. In addition, higher quality electron beams must be generated and transported to the wiggler. In general, all of the technologies became stressed as shorter wavelengths were approached.

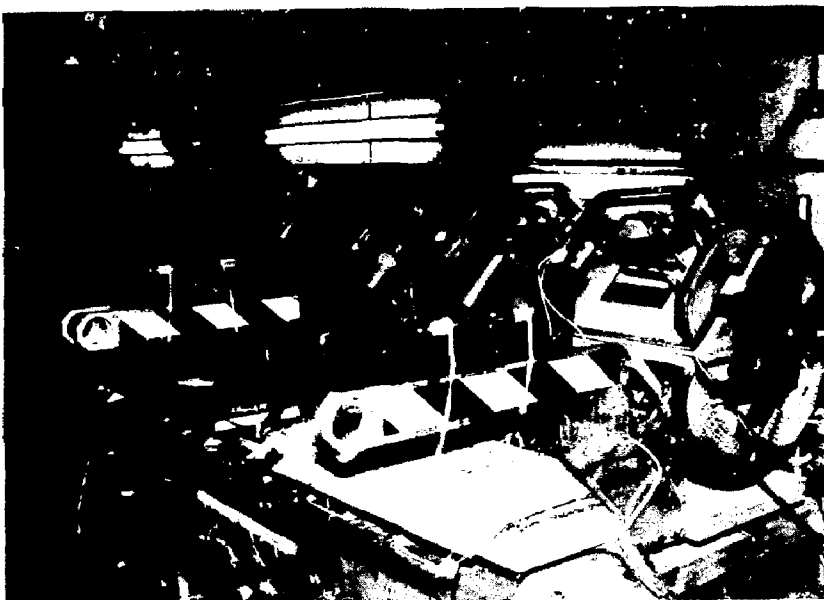


Figure 11. The ELF 3-m wiggler.

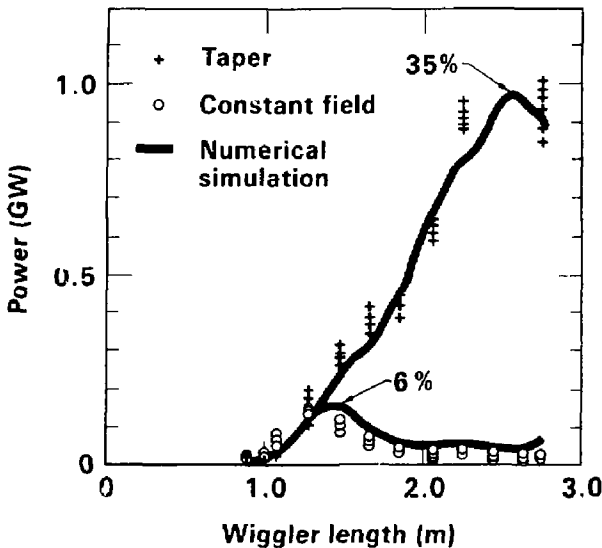


Figure 12. Results from the ELF experiment demonstrate the importance of a tapered wiggler.

The PALADIN experiment, now installed at our Advanced Test Accelerator (ATA), was designed to examine FEL physics at $10.6 \mu\text{m}$ in a long (25-m) wiggler (see Figs. 13 and 14). This experiment tests the performance of a single-pass wiggler in the regimes of both small and large signal gain. It will give opportunities to validate theoretical models of harmonic generation and will allow examination of the stability of the FEL amplifier against parasitic mechanisms such as sideband instability. We have measured the small signal gain with the first 5 m of the wiggler. At 15 m we have measured the gain of the amplifier and have demonstrated gain guiding. With a 14-kW input signal, and a 45-MeV electron beam, we have measured a gain of 27 dB (a factor of 500 between the input and output radiation signals). We have also observed gain guiding of the radiation, where diffraction losses are masked by the high gain of the FEL amplifier. The radiation signal in this case takes on the shape of the gain medium (electron beam). The signal is not saturated in this experiment; however, we have demonstrated saturation in the amplifier by increasing the input signal to 5 MW. The amplifier then saturates at roughly halfway through the wiggler. Numerical calculations have been successful in modeling these results. Currently we are experimenting with the full 25-m wiggler with the goal of measuring high gain extraction, optical guiding, and the spatial mode purity of the laser beam. Comparison with theoretical predictions is a key part of the experiment.

We are also planning a microwave FEL experiment on our new ETA-II accelerator, which will ultimately lead to heating of plasma in a tokamak fusion machine at LLNL.

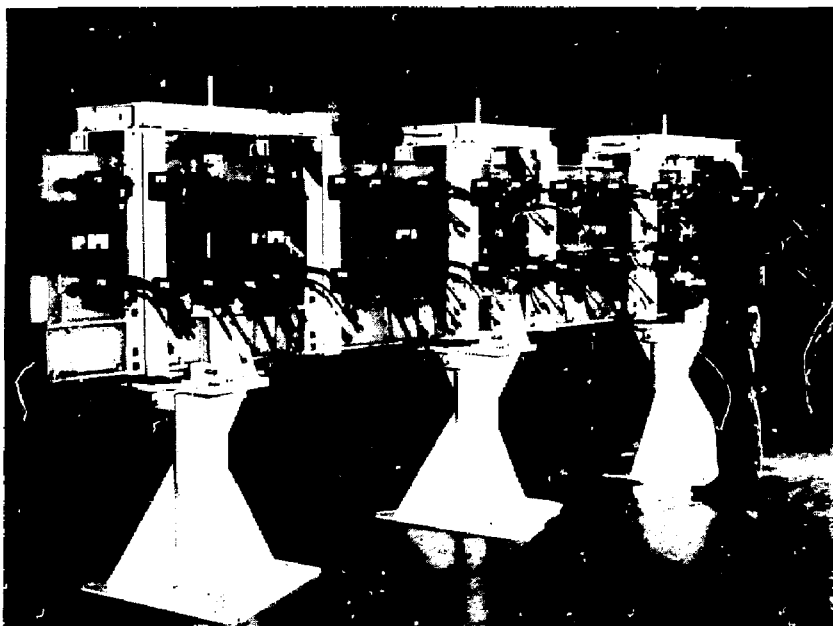


Figure 13. Five-meter section of the PALADIN wiggler.

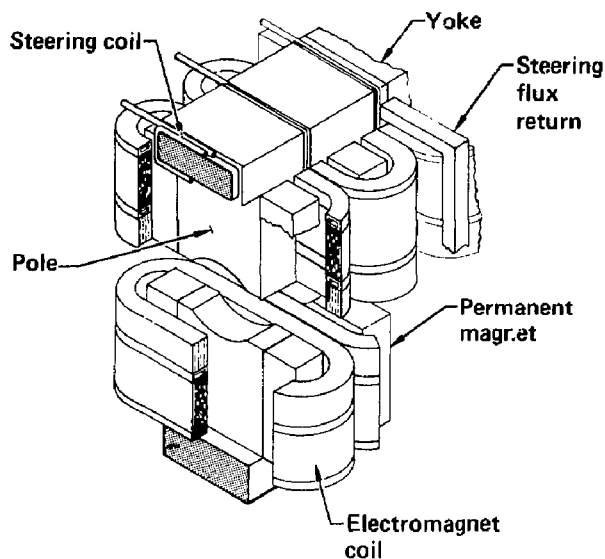


Figure 14. Cutaway of PALADIN wiggler showing poles, main electromagnetic windings, steering coils, and permanent magnet additions to the main pole pieces.

FEL Technology and Fusion Power

The desire to heat plasmas with high power microwaves at millimeter and submillimeter wavelengths may be fulfilled by the free electron laser. The FEL appears ideally suited for this application because it is capable of producing extremely high power and because it has a virtually limitless frequency range. Plasma heating is accomplished by tuning the FEL output frequency to a resonant frequency (cyclotron or twice cyclotron) of the plasma electrons. In a dense plasma, the resonant electrons will absorb the energy of the microwave field and rapidly transfer it to the other plasma particles. Besides having important implications for fusion-power technology, the application of the FEL to electron-cyclotron heating (ECH) may have an impact in other areas of plasma-physics research. The potential for using microwaves to heat plasmas has long been known but has been thwarted in scaling to higher magnetic fields and higher powers by the technology limits of the microwave-generating (gyrotron) tubes. As the frequency and power-per-unit requirements have grown, the tubes designed to heat plasma have become increasingly difficult and expensive to build. The advantage of FELs is that the high power per unit is an inherent feature of their design.

Experiments will be carried out at LLNL to demonstrate that FEL-generated microwaves can be used for both electron heating and current drive in tokamak plasmas. These experiments will address two issues simultaneously: determining how pulsing of the high-intensity field affects power absorption, and understanding the physics of the plasma response to high-power microwave heating.

For our planned experiments, we will use the new ETA II facility at LLNL and the Alcator-C tokamak, recently moved to LLNL from the Massachusetts Institute of Technology. The entire endeavor is called the Microwave Tokamak Experiment (MTX). We have begun the tokamak checkout and will begin microwave system checkout during early 1989. Heating experiments will follow.

A sketch of the facility (Fig. 15) shows the ECH experimental area containing the MTX and the ETA II, which contains the high-energy (7- to 10-MeV) electron-beam accelerator and the FEL wiggler. The electrical and electronic support equipment is not shown.

The MTX will be located just beyond the concrete shield that houses the ETA II. The output end of the FEL will then be situated approximately 19 m from the MTX. Power from the FEL will be transmitted to the tokamak through a quasi-optical, microwave transmission system, which would consist of a network of 0.6-m-diam ducts enclosing four mirrors that focus and direct the FEL microwave beam. The beam will be focused to enter the tokamak vacuum vessel through a narrow (4-cm) port.

Success in these experiments will demonstrate the usefulness of the FEL technology for driving and sustaining reactor plasmas. Good results will also provide a physics base for assessing the FEL's utility in devices for generating fusion power. If this technology fulfills its potential for driving current, controlling instabilities, and improving plasma confinement, ECH could become the method of choice for heating plasmas to ignition and for sustaining steady state plasma current in tokamaks.

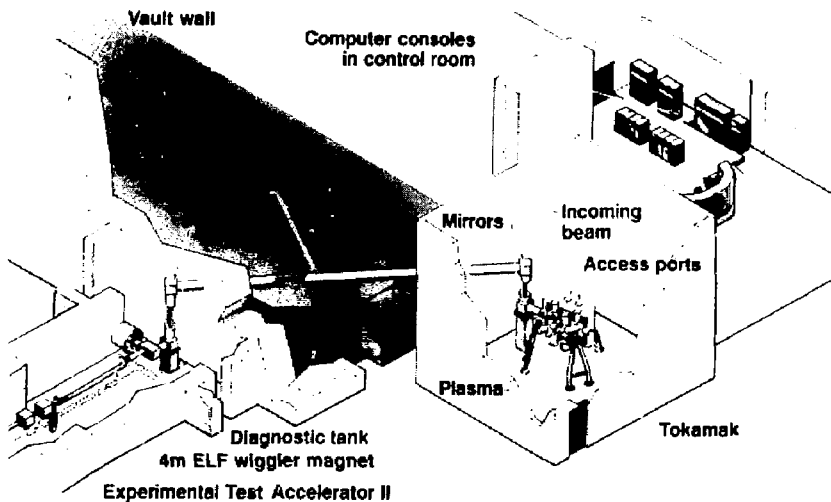


Figure 15. Sketch of the facility for the Microwave Tokamak Experiment (MTX). On the right is the tokamak machine in which the electron-cyclotron heating experiments will be carried out. On the left is the ETA II, containing the electron-beam accelerator and FEL wiggler.

FEL Technology and High Power Accelerators

A final application we wish to discuss is the application of FEL and induction accelerator technology to high power accelerators for high energy physics experiments.

As an alternate approach to the necessary high acceleration gradient via the relativistic klystron, discussed in Part A, we are proceeding with the concept of the two-beam accelerator (TBA), originally proposed by A.M. Sessler in 1982.⁵ In concept, the TBA employs a main high-energy-beam linear accelerator driven by a FEL, which runs parallel to it and serves as the power source for acceleration. The main accelerator, like that used at the Stanford Linear Accelerator Center (SLAC), is a disk-loaded waveguide powered by microwaves. The innovative feature of the TBA is that it uses an FEL, rather than klystrons or gyrotrons, as the source of the microwaves. With a TBA, power would be tapped off periodically along the FEL wiggler and fed across to the main accelerator. The FEL is designed so that its microwave power increase per unit length is equal to the average power extracted per unit length.

The advantage of employing the FEL—besides its relative simplicity—is its unique, inherent ability to generate economically very high power at very high frequencies. The simplicity of the FEL precludes the need for the thousands of individual microwave generators called for in conventional accelerator designs.

Although the advantage of operating at higher microwave frequencies has long been recognized, there have been no suitable high-power sources at about 1-cm wavelengths until the recent development of gyrotrons and FELs.

Gyrotrons are still being developed and may eventually prove to be a practical power source for some linear accelerators. However, their maximum power output at 1-cm wavelength seems likely to remain below 200 MW. Consequently, a 1-TeV machine would require thousands of such power sources, all properly locked in phase. Obviously, such a device would be impractical.

Our current theoretical and experimental work on the TBA is based on the FEL's ability to supply in excess of 1000 MW of average power at 1-cm wavelength. The TBA (Fig. 16) consists of a high-gradient, electron-beam-accelerator structure (HGS) periodically coupled to an FEL as a source of high-power microwave energy.

Interestingly, there is an inverse relationship between the basic functional concepts of the FEL and of the HGS: whereas the microwave field of the FEL wiggler obtains its drive power from an electron beam, the electron beam of the HGS obtains its drive power from a microwave field. This relationship has been likened to the operating principle of the transformer, wherein the microwave field is analogous to the transformer's magnetic coupling field.

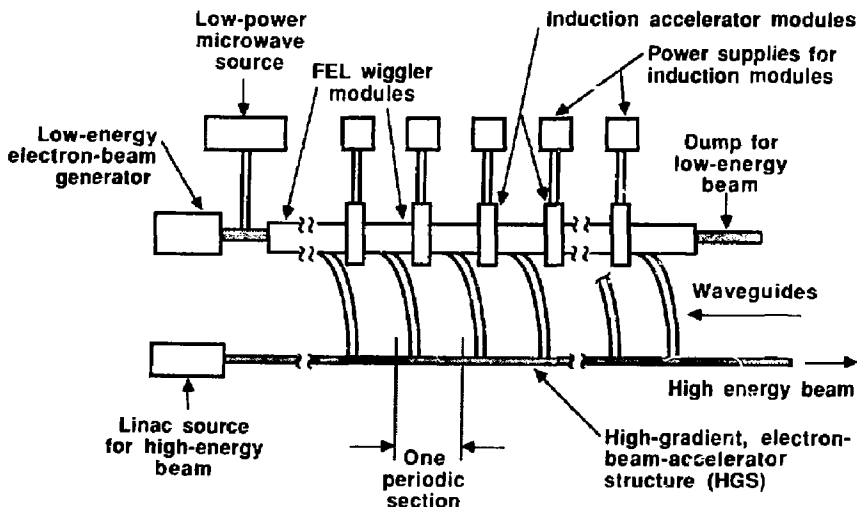


Figure 16. Diagram of the TBA concept. The TBA consists of a high-gradient, electron-beam accelerator structure (HGS) with a FEL wiggler running parallel to it and serving as its microwave-accelerating power source.

Although the FEL electron beam loses energy in the process of generating the high-power microwave field, the energy can be replenished by induction accelerator units placed periodically along the length of the FEL wiggler. The exact arrangement of the FEL driver to the high gradient accelerator, whether continuous along its length or modular, is still being evaluated.

Future research on the application of FELs in accelerators will be three pronged. First, we must optimize the design for the FEL's beam reacceleration cavity. Its overall beamline insertion length must probably be held to a few centimeters to avoid seriously degrading the TBA's high average acceleration gradient. Moreover, the microwave power loss in crossing the reacceleration gap should only be a few percent. Initial measurements of gap loss indicate that special focusing or guiding will be required to keep power loss down at an acceptable level.

Second, we must improve the luminosity of the beam. The desired high-energy beam luminosity is difficult to achieve when accelerating single electron bunches. The situation is mitigated by the acceleration of bursts of multiple bunches. This mode of operation has yet to be fully analyzed and optimized.

Third, we must address the issues of phase stability and control, perhaps the largest outstanding TBA design challenge. Analytical studies of the sensitivity of microwave phase to errors in operating parameters are proceeding at Lawrence Berkeley Laboratory. We require a phase-stabilizing scheme that is automatic and nearly instantaneous in response. We are continuing the search for a practical solution.

Summary

The current state of high-repetition-rate induction machine technology and of tapered wigglers is sufficient for near-term, high-average-power applications in the microwave and millimeter wavelength regimes. The additional physics demonstrations and developments needed for scaling the technology to shorter wavelengths is verification of the tapered wiggler operation in the optical wavelength regime, where "guiding" effects of the radiation are predicted to occur, and the generation and acceleration of very-high-brightness electron beams at multikiloampere current levels. Success in these two developments should open up a wide range of applications of this high-power FEL technology from millimeter to visible wavelengths.

ACKNOWLEDGMENT

The author would like to thank Samuel F. Eccles of the Beam Research Program, LLNL, for assembling and editing the material for this article.

REFERENCES

1. M. A. Allen, et al., "Relativistic Klystron Research and Development," presented at the European Particle Accelerator Conference, Rome, Italy, June 7-11, 1988.
2. A. M. Sessler and S. S. Yu, "Relativistic Klystron Two-Beam Accelerator," *Phys. Rev. Lett.* **58**, 2439 (1987).
3. T. J. Orzechowski, et al., "High Efficiency Extraction of Microwave Radiation from a Tapered Wiggler Free Electron Laser," *Phys. Rev. Lett.* **57**, 17 (1986).

4. N. M. Kroll, P. L. Morton, and M. N. Rosenbluth, "Free-Electron Lasers With Variable Parameter Wigglers," *IEEE J. Quantum Electron.* **QE-17** (1981); D. Prosnitz, A. Szoke, and V. K. Neil, "High-Gain, Free-Electron Laser Amplifiers: Design Considerations and Simulation," *Phys. Rev. A* **24**, 3 (1981).
5. A. M. Sessler, "The Free Electron Laser as a Power Source for a High-Gradient Accelerating Structure," in *Laser Acceleration of Particles* (AIP Conf. Proc. No. 91, American Institute of Physics, New York, 1982), pp. 154-159.